Influence of bar diameter on low-cycle fatigue degradation of reinforcing bars

Mohammad M. Kashani Ph.D., Shunyao Cai Ph.D., Sean A. Davis, Ph.D. and Paul J. Vardanega, Ph.D. M.ASCE

ABSTRACT

This note reports the results of 120 low-cycle fatigue tests on steel reinforcing bars with varying slenderness ratios at varying strain amplitudes. The failure modes of the fractured bars were investigated through analysis of the fractured mechanisms of bars. The results of experimental testing were used to update empirical models of low-cycle fatigue life for such bars. The newly improved empirical models were then incorporated into a recently developed constitutive material model, which accounts for bar buckling and fatigue. The experimental results show that the size effect is significant for short steel reinforcing bars where there is no buckling. The results also show that as the slenderness ratio of the steel reinforcing bars increases the influence of the bar diameter on low-cycle fatigue reduces.

Keywords: Inelastic buckling; Low-cycle fatigue; Size effect; Non-linear analysis; Stress-strain behaviour; Modelling

INTRODUCTION

For '*capacity design'* in earthquake engineering the designer aims to ensure the structure shows controlled ductility, to prevent collapse when it is subjected to large earthquakes. '*Capacity design*' for reinforced concrete (*RC*) structures is required by most current seismic design codes. The structure is designed for ductile failure at predictable locations known as *'plastic hinge'* regions. However, after large magnitude earthquakes, structures are not either functional or require significant repair. Considerable damage has been imparted on world cities due to recent large earthquakes (e.g., Christchurch in 2011: Kam and Pampanin, 2011; or the L'Aquila in 2012: Toniolo and Colombo,

2012), which can result in a significant fiscal loss to societies (Mander and Rodgers, 2015). Furthermore, the aim of performance-based seismic design and assessment of structures is to correlate damage to economic impact and therefore propose strategies to help mitigate risk (e.g., Moehle and Deierlein, 2004).

The nonlinear responses of reinforced concrete elements subject to repeated cyclic loading have been extensively investigated in previous research (e.g., CEB 1996). A key outcome of previous research is that inelastic buckling, and rupture of longitudinal reinforcement in RC components subject to cyclic loading are the primary failure mechanisms (e.g., El-Bahy et al. 1999; Lehman and Moehle, 2000.; Lee and Fenves, 1998; Zeris and Mahin, 1988; Neuenhofer and Filippou, 1997; Wehbe et al. 1999; Phan et al. 2007). Importantly there are many old infrastructure assets in regions of high seismicity not designed for earthquake loading. Therefore, these structures have often been poorly detailed and are not capable of accommodating large plastic deformation in plastic hinge regions. Experience from past major earthquakes and experimental testing (Mander and Rodgers, 2015; Lehman and Moehle, 2000 and Phan et al. 2007) showed that inelastic buckling of longitudinal reinforcement and subsequently premature concrete crushing due to compression is the main failure mode of old structures. Other researchers (Brown and Kunnath 2000 and 2004; Kashani et al. 2013a; Kashani et al. 2015a and Kunnath et al. 2009) reported that inelastic buckling shorten the low cycle fatigue (LCF) (at high amplitude) life of the reinforcement.

Several researchers investigated the low-cycle high amplitude fatigue and nonlinear cyclic behaviour of bars with and without the influence of inelastic buckling (Kunnath et al. 2009; Monti and Nuti, 1992; Gomes and Appleton, 1997; Rodriguez et al. 1999; Dhakal and Maekawa, 2002; Kashani, 2013a and 2013b; Mander et al. 1994; Brown and Kunnath, 2004; Higai et al. 2006 and Hawileh et al. 2010). More recently Kashani et al. (2015a) and Kashani et al. (2016) investigated the effect of inelastic buckling on *LCF* performance of steel reinforcement and its impact on nonlinear

flexural response of RC bridge piers subject to repeated cyclic loading: reporting that inelastic buckling negatively impacts on *LCF* performance of steel reinforcement bars.

Study Aims

Kashani et al (2015a) studied degradation due to LCF at high amplitude of 12mm and 16mm steel reinforcing bars (effectively constant diameter). Kashani et al (2015b) presented the constitutive model used in this note which was originally calibrated using the data reported in Kashani et al (2015a). Kashani (2017) studied the influence of bar diameter (*D*) on inelastic buckling behaviour of corroded steel reinforcement loaded in monotonic compression neglecting fatigue effects. Gehlen et al. (2016) investigated the influence of corrosion and *D* on high-cycle fatigue behaviour of reinforcing bars. Kashani et al. (2018b) used a parametric study to assess the influence of various factors affecting the nonlinear flexural response of rectangular *RC* columns (component level). Kashani et al. (2015a and 2018b) posited that *D* may affect the *LCF* performance of reinforcement. This note aims to determine if *D* influences the *LCF* performance of steel reinforcement allowing for inelastic buckling.

Methodology

The experimental programme involved testing steel reinforcement with varying *D* and slenderness ratio (*L*/*D*) under cyclic strain history with varying strain amplitudes. The experimental methodology is similar to that presented in Kashani et al. (2015a). The failure mechanism of the fractured bars is investigated through analyses of the ruptured surfaces using the scanning electron microscope (*SEM*) images. The results of experimental testing were used to update existing empirical models (e.g., Mander et al. 1994; Brown and Kunnath, 2004) to study the effect of *D* on the *LCF* life of reinforcing bars. The updated empirical models were then incorporated in the uniaxial constitutive material model for steel bars (developed by Kashani et al. ,2015b) also implemented in OpenSees (OpenSees, 2014).

TESTING PROGRAMME

120 test specimens with varying D and L/D were produced for the experimental programme. The tested samples included 30x10mm diameter, 30x12mm diameter, 30x16mm diameter, and 30x20mm diameter reinforcing bars with varying slenderness ratio (5, 8, 10, 12 and 15). For each set of bar diameters three tension tests were conducted to characterise the material properties of the bars (see Kashani 2017 for further details as the material used in the experiments reported here is the same as in that used in the study of Kashani 2017).

The experimental testing apparatus is the same as that used in Kashani et al. (2015a), and therefore, for brevity, is not discussed here. The complete rupture of bars was identified as the failure point of test specimen and end of the test. See Tables S1 to S4 for the experimental results.

EXPERIMENTAL RESULTS

Influence of *D* on hysteretic loops

The measured cyclic stress-strain hysteretic responses of the test specimens with L/D = 5 and L/D = 15 with D varying are shown in Figure 1 (in Figure 1, the stress (σ) in the y axis normalised with yield stress (σ_y)). The experimental results (Figure 1) show qualitatively that the D has some influence on hysteretic stress-strain behaviour of bars of L/D = 5. As the L/D ratio of the bars increases (cf. the results for L/D = 15) the influence of D reduces, due to the influence of plasticity on the hysteretic response (Figure 1b). Inelastic buckling initiates when three plastic hinges occur along the length of bars (Kashani, 2013b). In short bars, the ratio of elastic length (elastic region between plastic hinges) to plastic hinge length is minimal. In very short bars ($L/D \leq 6$) almost the whole bar length goes plastic. Therefore, the three dimensional effect due to material dislocation (molecular response) has an influence on the global response under repeated cyclic loading (cyclic stress-strain). As L/D increases the behaviour tends more towards nonlinear beam-column behaviour, and geometrical nonlinearity (buckling effect) is governing the global response.

Influence of *D* on plastic energy dissipation

The influence of D on *LCF* degradation of the reinforcement is examined quantitatively in this section. The total plastic hysteretic energy dissipated during testing is used as a measure of the damage. The calculated plastic energy (normalised) dissipated in each test is shown in Figure 2. The total hysteretic energy is denoted as E_t and the elastic energy when the specimen is subjected to monotonic tensile testing is denoted as E_y. Figure 2 shows that as the strain amplitude of the cyclic test increases the influence of D on normalised dissipated energy increases and the group of steel bars where $L/D = 5$ and $L/D = 8$ are most affected by varying D. However, the energy plots do not show a systematic pattern between the D and the normalised plastic energy dissipated. Increasing L/D decreases the influence of D on dissipated energy. Figure 2 shows that when $L/D >$ approximately 10, D has minimal influence. This is in line with results observed in previous studies by Chang and Mander (1994), Kashani et al. (2013a), Kashani et al. (2015c) and Kashani (2017). However, in none of the previous studies the influence of D investigated for a wider range of D and L/D.

ANALYSIS OF FRACTURED SURFACE USING SEM

A JSM IT300 SEM was used for the investigation of the fracture mechanism of the tested bars subjected to repeated cyclic loading. SEM high-resolution detailed images of the topography of the fractured surfaces of tested specimens were taken.

Figure 3 shows the fractographs of some tested bars with $L/D = 5$ (which did not buckle) with varying diameter at 4% strain amplitude. Comparison of Figure 3(a) and (b) with Figure 3(c) and (d) reveals darker areas of ridges caused by straining which are due to slower crack propagation (when $D = 10$mm) (NB. The specimens shown in Figures 3a and 3b fractured later and exhibited increased plastic deformation cf. Figure 2). Examination of Figure 3 (c) and (d) reveal lighter areas which indicate more sudden fracture events, indicating D has some influence on the fracture mechanism.

The fractographs for the 12mm and 16mm bars are given as Figure S1. Figure S2 shows some fractographs for the L/D = 15 specimens (with buckling effect) and various diameters at 4% strain amplitudes. Figure S2 (unlike Figures 3 and S1) shows a brittle fracture in all bars regardless of their diameter, indicating that once bars buckle the strain amplitude is locally increased due to large deformation. Therefore, the crack growth is faster, and D does not significantly influence the performance of these bars.

To qualitatively investigate the material composition of tested specimens, energy-dispersive X-ray spectroscopy (EDX) is conducted using SEM. This is to check that the differences observed in the fatigue life of tested bars are purely due to D, and is not related to any materials composition. Figure S3 shows the spectra of tested specimens. The tested specimens are B500C British manufactured bars according to BSI (2016) with controlled chemical composition, which requires a carbon equivalent of less than 0.50% to be code compliant, when calculated according to BSI (2016). Figure S3 shows that the main component of these bars is Iron (Fe), indicating insignificant material variation which is judged not to influence the experimental results reported in this note.

MODELLING LOW-CYCLE PERFORMANCE OF REINFORCING STEEL INCLUDING THE COMBINED EFFECTS OF INELASTIC BUCKLING AND BAR DIAMETER

Using the Koh-Stephen model (Koh and Stephens, 1991), Kashani et al. (2015a) investigated the effect of inelastic buckling on *LCF* degradation of reinforcement. Koh-Stephen's model (Koh and Stephens, 1991) uses total strain amplitude (i.e. the sum of elastic and plastic strain) (in lieu of plastic strain amplitude) to carry out fatigue life calculations.

Koh-Stephen's model is described in Eq. (1) (see Koh and Stephen 1991):

$$\varepsilon_a = \varepsilon_f \left(2N_f\right)^{\alpha} \tag{1}$$

To quantify the fatigue parameters (εf, α), Eq. (1) is fitted to the fatigue test data for each L/D and D individually. Table 1 shows the results of the regressions and the corresponding $p_{0.05}$ values. Figure 4

shows Equation (1) fitted to some of the individual data-sets. After calibration of, ε_f and α, for each group of bars, the influence of inelastic buckling on these parameters was explored using further regression analysis.

Influence of inelastic buckling on LCF parameters

Many researchers have studied the influence of inelastic buckling on the stress-strain response of steel reinforcement when loaded in monotonic and cyclic fashions (Monti and Nuti, 1992; Gomes and Appleton, 1997; Rodriguez et al. 1999; Shakal and Maekawa, 2002; Kunnath et al. 2009; Kashani et al. 2013a and Kashani et al. 2014), and confirmed that σ_y, and L/D are the most influential parameters of inelastic buckling (and post-buckling) behaviour. Dhakal and Maekawa (2002) defined a bar buckling parameter λ_p, by Eq. (2) (yield stress in Eq. 2 is in MPa):

$$\lambda_p = \sqrt{\frac{\sigma_y}{100}}\frac{L}{D} \tag{2}$$

Kashani et al. (2015a) showed that the relationship between (εf, α) and λ_p is statistically significant, which supported by the results presented in this note. However, the results that were reported in Kashani et al. (2015a) are based on experimental data of 12mm and 16mm diameter bars. In this note the previous results are extended to investigate the effect of D.

The relationship between fatigue parameters (εf, α) and the λ_p was determined by regression. The effect on (ε_f, α) of inelastic buckling can be modelled using the empirical Eqs. (3) and (4).

$$\alpha = a\,\lambda_p + b \tag{3}$$

$$\varepsilon_f = c\exp\left(d\,\lambda_p\right) \tag{4}$$

A negative correlation was observed between α and λ_p. Comparison of the regression graphs (Figure 5) indicates that the D has some influence on the slope of best fit line. The regression analyses also reveal a positive exponential correlation between the ε_f and λ_p, (also observed in Kashani et al. 2015a although in the previous study D values of 12mm and 16mm were used).

Influence of *D* on LCF material constants

The influence of varying D on the fatigue parameters (ε_f, α) is explored. The regression analyses results show no significant between the D and a and d (see Table 2) as indicated by p-values greater than 0.05. Figure 5 shows the interrelationship between b and c, and D. The p-values of fitted coefficients in Figure 5 at 0.05 significance are less than 0.05, which confirms a strong correlation between D and coefficients b and c.

The regression analysis indicate that D does not affect the slope of the straight line implied by Eq. 3 and also that D does not affect the exponent in Eq. 4, this suggesting that D does not directly affect λ_p. Therefore, based on the results in this note, as L/D increases the influence of D on fatigue material coefficients reduces. If the bars are affected by inelastic buckling varying D should not affect the resulting *LCF* life which is mainly governed by varying λ_p.

Due to capacity limitations of the Instron machine available, a larger range of D could not be tested. A larger range of D values may reveal different trends to those shown in this note. An important question may be posed: do the, currently available uniaxial material models apply at a wider range of vales of D? With this in mind further analyses were conducted to compare the experimental results with a hysteretic material model, as described in the next section.

SIMULATIONS

Kashani et al. (2015b) established a new constitutive model for reinforcing bars can that account for both buckling and *LCF*. The details of model verification and experimental validation, and more recent development of the model to incorporate the influence of buckling on *LCF* material parameters are discussed in previous publications (Kashani et al. 2013a, Kashani et al. 2013b, Kashani et al. 2015a). The model suggested by Kashani et al. (2015b) was updated and compared with the new test data. The comparison between the enhanced analytical model using the new fatigue

parameters (ε_f, α) (discussed in this note) and the experimental results are shown qualitatively in Figure 6 for the 20mm bars (the results for the other diameters are given as Figure S4).

The computed and experimental normalised dissipated energy of all bars with $L/D \geq 8$ are plotted at small and large strain amplitudes in Figure 7. Furthermore, the mean and standard deviation of the normalised energy values for small and large-strain amplitudes are also plotted in Figure 8. Figures 7 and 8 show that from the constitutive model can adequately simulate the nonlinear cyclic stress-strain behaviour and predict the LCF failure of reinforcing bars allowing for the effects of both inelastic buckling and D.

SUMMARY

A set of 120 fatigue tests with constant amplitudes were conducted on steel bars with varying L/D and D. Using *SEM*, the fracture mechanisms of fractured surfaces were studied, and chemical material composition of test specimens were investigated. Using the experimental data, the correlation between *LCF* model parameters and inelastic buckling and D was explored. Finally, the proposed empirical models were incorporated in to a previously published constitutive model (Kashani et al. 2015b) to simulate the nonlinear stress-strain relations of steel bars.

The summary findings of this note are:

a) The analysis of ruptured bars using SEM method showed that as D increased in bars with $L/D = 5$ the failure mode became more brittle. However, as the L/D of bars increased ($L/D \geq 10$) almost all the bars with different D vales exhibited similar failure modes.

b) The experimental fatigue tests revealed that as D increases reinforcing bars fracture earlier under repeated cyclic loading. The D affects the *LCF* performance of steel bars. Increasing the L/D ratio appears to reduce the influence of D on LCF performance of these bars.

c) For short bars ($L/D \leq$ approximately 6), inelastic buckling is not critical, D has a considerable influence on LCF life steel reinforcing bars. However, the *LCF* performance of bars affected by inelastic buckling is mainly governed by their bar buckling parameter, λ_p (a function of L/D and σ_y).

DATA AVAILABILIY STATEMENT

The raw test data from the *LCF* tests is available from Kashani et al. (2018a).

ACKNOWLEDGEMENTS

The experimental programme was financially supported by the Earthquake and Geotechnical Engineering Research Group (EGERG) at the University of Bristol. The SEM studies were conducted in the Chemistry Imaging Facility with equipment funded by the University of Bristol and the Engineering and Physical Sciences Research Council grant number EP/K035746/1. The third author is thankful for the financial support provided by China Scholarship Council (File No. 201506260126). Any recommendations provided in this note are the opinions of the authors and do not constitute a standard or code of practice. The authors thank the anonymous reviewers for their help improving the note.

NOTATION

The following symbols are used in this note:

a, b, c, d = regression coefficients;

D = bar diameter;

E_y = elastic energy under monotonic tension;

E_t = total hysteretic energy;

L = length of steel reinforcing bar;

L/D = slenderness ratio;

$2N_f$ = number of half-cycles to failure;

p = p-value;

$p_{0.05}$ = p-value at 0.05 significance level;

R^2 = coefficient of determination;

α = ductility exponent;

ε_{ap} = strain amplitude;

ε_f = ductility coefficient (fracture strain due to one load reversal);

ε_y = yield strain;

λ_p = non-dimensional bar buckling parameter;

μ = mean;

σ = stress (or standard deviation);

σ_y = yield stress.

SUPPLEMENTAL DATA

The online supplemental data which contains Tables S1 to S4 and Figures S1 to S4 is available online in the ASCE Library (www.ascelibrary.org).

REFERENCES

Brown, J. and Kunnath, S. K. (2000). Low cycle fatigue behavior of longitudinal reinforcement in reinforced concrete bridge columns. *Technical Report MCEER-00-0007*, Multidisciplinary Centre for Earthquake Engineering Research, University at Buffalo, State University of New York, New York, USA. https://ubir.buffalo.edu/xmlui/bitstream/handle/10477/788/00-3580007.pdf?sequence=3 (accessed 10 September 2018).

Brown, J. and Kunnath S. K. (2004). Low-cycle fatigue failure of reinforcing steel bars. *ACI Materials Journal*, **101(6):** 457-466.

BSI (British Standards Institution) (2016) BS 4449-2005+A3:2016 Steel for the reinforcement of concrete - Weldable reinforcing steel - bar, coil and decoiled product – Specification. British Standards Institution, London, UK.

Comite Euro-International Du Beton (CEB) (1996). RC Elements Under Cyclic Loading – State-of-the-art Report. Thomas Telford, London, United Kingdom. ISBN: 0-7277-2086-4.

Chang, G. A. and Mander, J. B. (1994). Seismic energy based fatigue damage analysis of bridge columns: Part I – Evaluation of seismic capacity. Technical report NCEER-94-0006, 1994. https://ubir.buffalo.edu/xmlui/bitstream/handle/10477/851/94-0006.pdf?sequence=3 (accessed 10 September 2018).

Dhakal, R and Maekawa, K. (2002). Path-dependent cyclic stress-strain relationship of reinforcing bar including buckling. *Engineering Structures*, **24(11):** 1139–1147, https://doi.org/10.1016/S0141-0296(02)00080-9.

El-Bahy, A., Kunnath, S. K, Stone, W. C. and Taylor, A. W. (1999). Cumulative Seismic Damage of Circular Bridge Columns: Benchmark and Low-Cycle Fatigue Tests. *ACI Structural Journal*, **96(4):** 633-643.

Gehlen, C., Osterminski, K. and Weirich, T. (2016). High-cycle fatigue behaviour of reinforcing steel under the effect of ongoing corrosion. *Structural Concrete*, **17(3):** 329-337, https://doi.org/10.1002/suco.201500094.

Gomes, A. and Appleton J. (1997). Nonlinear cyclic stress-strain relationship of reinforcing bars including buckling. *Engineering Structures*, **19(10):** 822-826, https://doi.org/10.1016/S0141-0296(97)00166-1.

Hawileh, R. A., Abdalla, J. A., Oudah, F. and Abdelrahman, K. (2010). Low-cycle fatigue life behaviour of BS 460B and BS B500B steel reinforcing bars. *Fatigue and Fracture of Engineering Materials and Structures*, **33(7):** 397-407, https://doi.org/10.1111/j.1460-2695.2010.01452.x.

Higai T, Nakamura H and Saito S. (2006). Fatigue failure criterion for deformed bars subjected to large deformation reversals. Chapter 4 - *ACI Special Publication 237 Finite Element Analysis of Reinforced Concrete Structures,* ISBN: 9780870312151, pp. 37-54.

Kam, W. Y. and Pampanin, S. (2011). The seismic performance of RC buildings in the 22 February 2011 Christchurch earthquake. *Structural Concrete*, **12(4):** 223-233, https://doi.org/10.1002/suco.201100044.

Kashani, M. M., Cai, S., Davis, S. A. and Vardanega, P. J. (2018a). *Supporting Data for 'Influence of bar diameter on low-cycle fatigue degradation of reinforcing bars'* University of Bristol, Bristol, UK, http://dx.doi.org/10.5523/bris.1kz5015zjoel92ueb97kwxd4ps

Kashani, M. M., Salami, M. R., Goda, K., and Alexander, N. A. (2018b). Non-linear flexural behaviour of RC columns including bar buckling and fatigue degradation. *Magazine of Concrete Research*, **70(5):** 231-247, https://doi.org/10.1680/jmacr.16.00495.

Kashani, M. M., Crewe, A. J. and Alexander, N. A. (2013a). Nonlinear cyclic response of corrosion-damaged reinforcing bars with the effect of buckling. *Construction and Building Materials*, **41:** 388-400, https://doi.org/10.1016/j.conbuildmat.2012.12.011.

Kashani, M. M., Crewe, A. J. and Alexander, N. A. (2013b). Nonlinear stress–strain behaviour of corrosion damaged reinforcing bars including inelastic buckling. *Engineering Structures*, **48:** 417-429, https://doi.org/10.1016/j.engstruct.2012.09.034.

Kashani, M. M., Lowes, L. N., Crewe, A. J. and Alexander, N. A. (2014). Finite element investigation of the influence of corrosion pattern on inelastic buckling and cyclic response of corroded reinforcing bars. *Engineering Structures*, **75:** 113-125, https://doi.org/10.1016/j.engstruct.2014.05.026.

Kashani, M. M., Barmi, A. K., and Malinova, V. S. (2015a). Influence of inelastic buckling on low cycle fatigue degradation of reinforcing bars. *Construction and Building Materials*, **94:** 644-655, https://doi.org/10.1016/j.conbuildmat.2015.07.102.

Kashani, M. M., Lowes, L.N., Crewe, A. J. and Alexander, N. A. (2015b). Phenomenological hysteretic model for corroded reinforcing bars including inelastic buckling and low-cycle fatigue degradation. *Computers and Structures*, **156:** 58-71, https://doi.org/10.1016/j.compstruc.2015.04.005.

Kashani, M. M., Alagheband, P., Khan, R. and Davis S. (2015c). Impact of corrosion on low-cycle fatigue degradation of reinforcing bars with the effect of inelastic buckling. *International Journal of Fatigue*, **77:** 174-185, https://doi.org/10.1016/j.ijfatigue.2015.03.013.

Kashani, M. M., Lowes, L. N., Crewe, A. J. and Alexander, N. A. (2016). Nonlinear fibre element modelling of RC bridge piers considering inelastic buckling of reinforcement. *Engineering Structures*, **116:** 163-177, https://doi.org/10.1016/j.engstruct.2016.02.051.

Kashani, M. M. (2017). Size effect on inelastic buckling behavior of accelerated pitted corroded bars in porous media. *Journal of Materials in Civil Engineering (ASCE)*, **29(7):** 04017022, https://doi.org/10.1061/(ASCE)MT.1943-5533.0001853.

Koh, S. K. and Stephens, R. I. (1991). Mean Stress Effects on Low Cycle Fatigue for a High Strength Steel. *Fatigue and Fracture of Engineering Materials and Structures*, **14(4):** 413-428.

Kunnath, S. K., Heo, Y. and Mohle, J. F. (2009). Nonlinear uniaxial material model for reinforcing steel bars. *Journal of Structural Engineering (ASCE)*, **135(4):** 335-343, https://doi.org/10.1061/(ASCE)0733-9445(2009)135:4(335).

Lee, J. and Fenves, G. L. (1998). Plastic-damage model for cyclic loading of concrete structures. *Journal of Engineering Mechanics (ASCE),* **124(8):** 892-900, https://doi.org/10.1061/(ASCE)0733-9399(1998)124:8(892).

Lehman, D. E. and Moehle, J. P. (2000). Seismic Performance of Well-Confined Concrete Columns. PEER Report 1998/01, Pacific Earthquake Engineering Research Center, College of Engineering, University of California, Berkeley, CA, United States. Available from:

https://apps.peer.berkeley.edu/publications/peer_reports/reports_1998/9801.pdf (accessed 10 September 2018)

Mander, J. B., Panthaki, F. D., and Kasalanati, A. (1994). Low-cycle fatigue behavior of reinforcing steel. *Journal of Materials in Civil Engineering (ASCE)*, **6(4):** 453-468, https://doi.org/10.1061/(ASCE)0899-1561(1994)6:4(453).

Mander, J. B. and Rodgers, G. W. (2015). Analysis of low cycle fatigue effects on structures due to the 2010-2011 Canterbury earthquake sequence. *Proceedings of the Tenth Pacific Conference on Earthquake Engineering – Building and Earthquake Resilient Pacific*. 6-8 November 2015, Sydney, Australia. Available from: http://www.aees.org.au/wp-content/uploads/2015/12/Paper_113.pdf (accessed 10 September 2018).

Moehle, J. P. and Deierlein, G. G. (2004). A framework methodology for performance-based earthquake engineering. Paper presented at *13th World Conference on Earthquake Engineering*, Vancouver, B.C. Canada, August 1-6, 2004. Paper No. 679. Available from: http://www.iitk.ac.in/nicee/wcee/article/13_679.pdf (accessed 10 September 2018).

Monti, G. and Nuti, C. (1992). Nonlinear cyclic behavior of reinforcing bars including buckling. *Journal of Structural Engineering (ASCE)*, **118(12):** 3268–3284, https://doi.org/10.1061/(ASCE)0733-9445(1992)118:12(3268).

Neuenhofer, A. and Filippou, F. C. (1997). Evaluation of nonlinear frame finite-element models. *Journal of Structural Engineering (ASCE)*, **123(7):** 958-966, https://doi.org/10.1061/(ASCE)0733-9445(1997)123:7(958).

OpenSees, the Open System for Earthquake Engineering Simulation. (2014), PEER 2011; University of California, Berkeley, CA, United States (http://opensees.berkeley.edu/) (accessed 10 September 2018).

Phan, V., Saiidi, M. S., Anderson, J. and Ghasemi, H. (2007). Near-fault ground motion effects on reinforced concrete bridge columns. *Journal of Structural Engineering (ASCE*), **133(7):** 982-989, https://doi.org/10.1061/(ASCE)0733-9445(2007)133:7(982).

Rodriguez, M. E., Botero, J. C. and Villa J. (1999). Cyclic stress-strain behavior of reinforcing steel including the effect of buckling. *Journal of Structural Engineering (ASCE)*, **125(6):** 605–612, https://doi.org/10.1061/(ASCE)0733-9445(1999)125:6(605).

Toniolo, G. and Colombo, A. (2012). Precast concrete structures: the lessons learned from the L'Aquila earthquake. *Structural Concrete*, **13(2):** 73-83, https://doi.org/10.1002/suco.201100052.

Wehbe, N. I., Saiidi, M. S. and Sanders, D. H. (1999). Seismic performance of rectangular bridge columns with moderate confinement. ACI *Structural Journal*, **96(2):** 248-258.

Zeris, C. A. and Mahin, S. A. (1988). Analysis of reinforced concrete beam-columns under uniaxial excitation. *Journal of Structural Engineering (ASCE)*, **114(4):** 804-820, https://doi.org/10.1061/(ASCE)0733-9445(1988)114:4(804).

Table 1: Calibrated low-cycle fatigue parameters (ε_f, α)

10 mm Diameter Bars					
L*/*D	5	8	10	12	15
ε_a	0.190	0.184	0.312	0.357	0.350
α	-0.457	-0.537	-0.689	-0.721	-0.695
p-value	0.0089	0.0014	0.0012	0.0016	0.0014
λ_p	11.619	18.590	23.238	27.885	34.857
12 mm Diameter Bars					
L*/*D	5	8	10	12	15
ε_a	0.190	0.189	0.245	0.341	0.354
α	-0.443	-0.542	-0.613	-0.725	-0.733
p-value	0.0011	0.0016	0.0011	0.0017	0.0018
λ_p	11.619	18.590	23.238	27.885	34.857
12 mm Diameter Bars					
L*/*D	5	8	10	12	15
ε_a	0.131	0.157	0.206	0.316	0.376
α	-0.399	-0.506	-0.615	-0.719	-0.748
p-value	0.0016	0.0273	0.0099	0.0014	0.0107
λ_p	11.511	18.417	23.022	27.626	34.533
20 mm Diameter Bars					
L*/*D	5	8	10	12	15
ε_a	0.150	0.152	0.227	0.227	0.401
α	-0.410	-0.479	-0.607	-0.610	-0.766
p-value	0.0010	0.0013	0.0022	0.0012	0.0019
λ_p	11.511	18.417	23.022	27.626	34.533

NB the p-values are those computed when Eq. 1 is fitted.

Table 2: Calibrated fatigue parameters (ε_f, α) as a function of the λ_p

Material constants	*a*	*b*	*c*	*d*
10 mm diameter bars				
α	-0.010	-0.384		
ε_f			0.142	0.028
p-value	0.0021	0.0017	0.0030	0.0040
12 mm diameter bars				
α	-0.010	-0.364		
ε_f			0.146	0.023
p-value	0.0041	0.0027	0.0130	0.0140
16 mm diameter bars				
α	-0.010	-0.333		
ε_f			0.122	0.021
p-value	0.0042	0.0051	0.001	0.001
20 mm diameter bars				
α	-0.015	-0.223		
ε_f			0.066	0.051
p-value	0.0022	0.0410	0.0044	0.0103

NB the p-values are those computed when Eq. 3 and 4 are fitted.

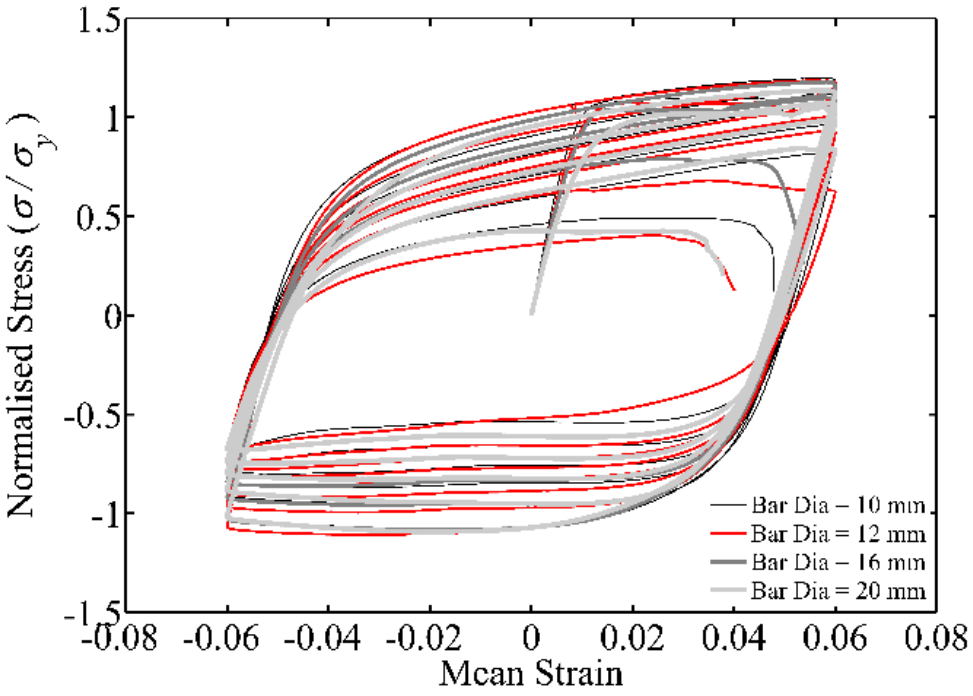

(a)

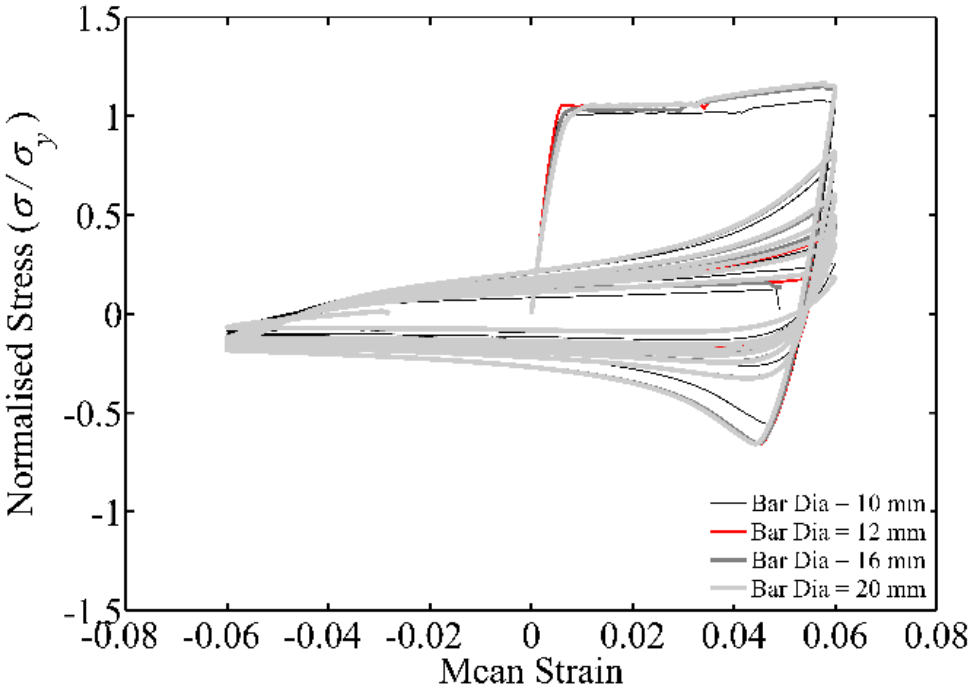

(b)

Figure 1: Influence of bar diameter on stress-strain behaviour of reinforcing bars with and without the effect of buckling: (a) L/D = 5 at 6% strain amplitude, and (b) L/D = 15 at 6% strain amplitude

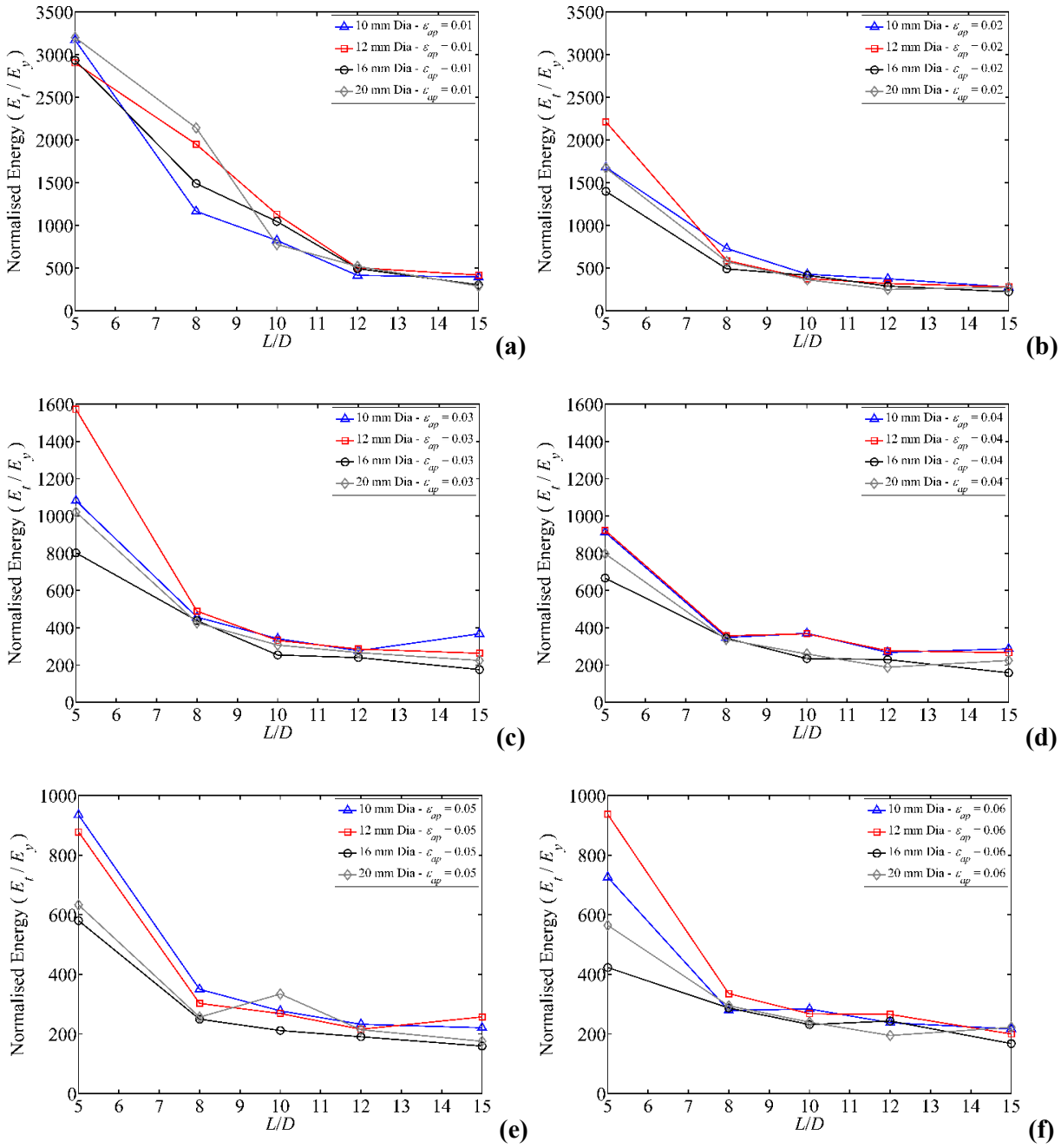

Figure 2: Influence of bar diameter on total plastic energy dissipation of reinforcing bars with various slenderness ratios: (a) 1% strain amplitude, (b) 2% strain amplitude, (c) 3% strain amplitude, (d) 4% strain amplitude, (e) 5% strain amplitude, and (f) 6% strain amplitude

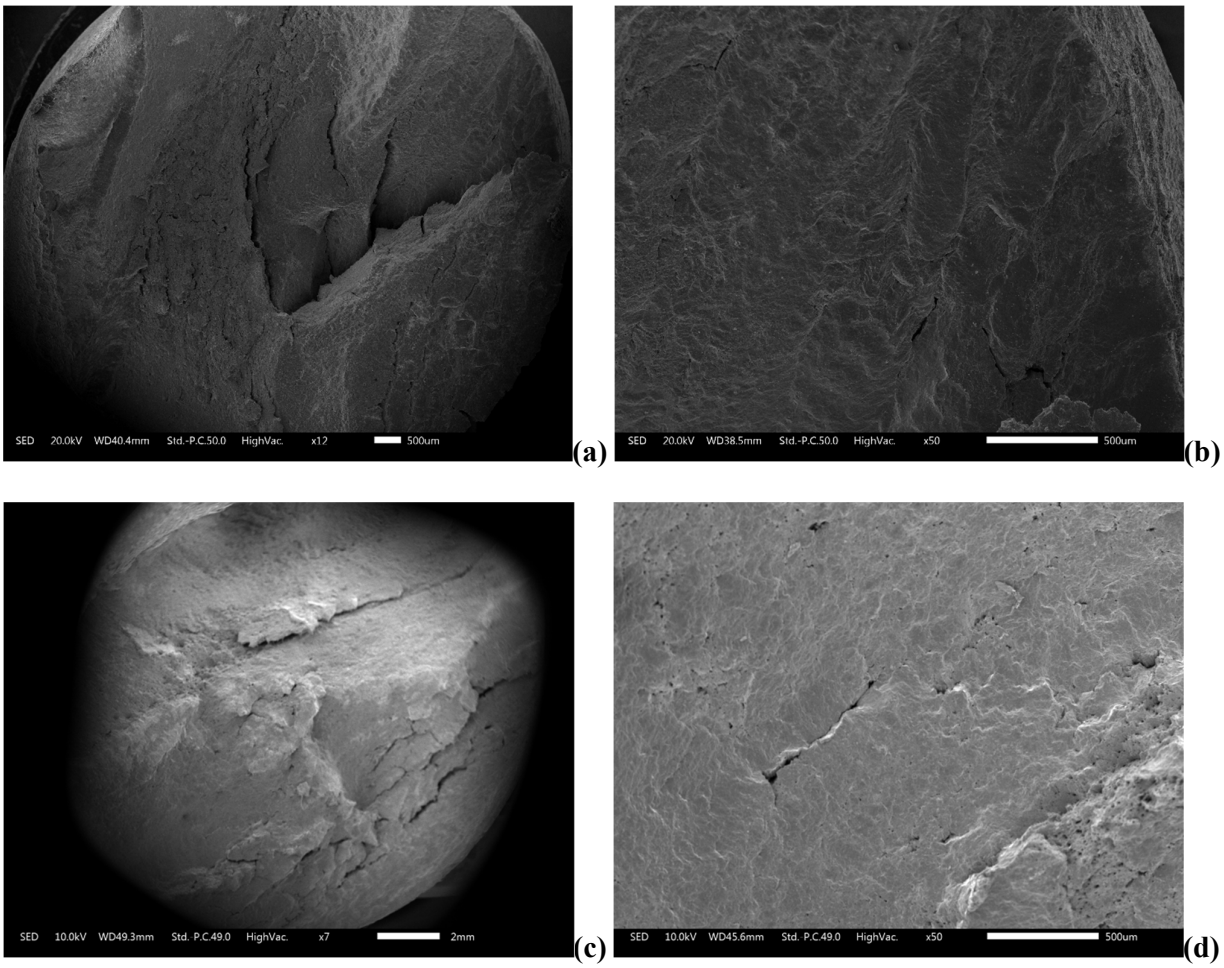

Figure 3: SEM fractographs of fractured bars without the effect of buckling with L/D = 5: (a) and (b) 10 mm diameter at 4% strain amplitude, and (c) and (d) 20 mm diameter at 4% strain amplitude

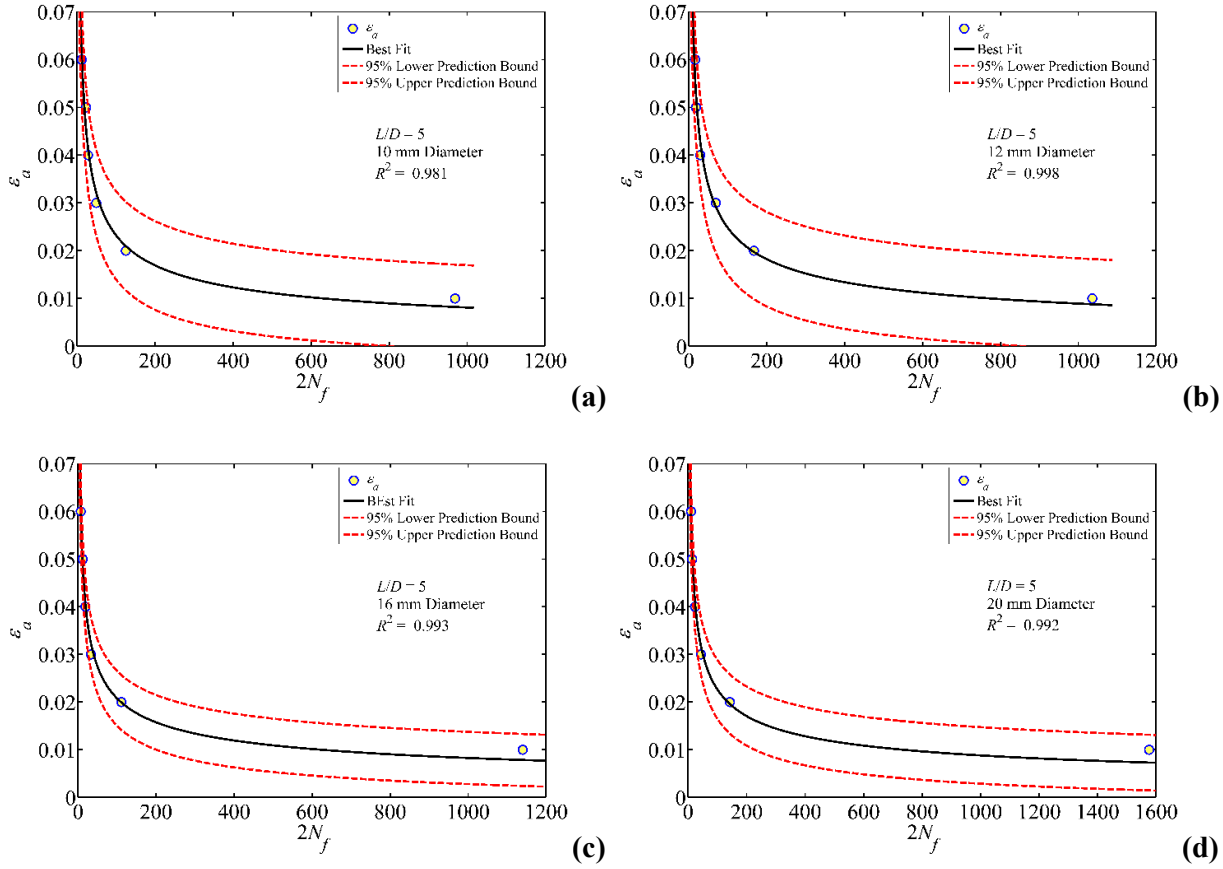

Figure 4: Examples of calibrating fatigue materials constants by fitting Koh-Stephen (Koh and Stephens, 1991) model: (a) L/D = 5, 10 mm diameter (b) L/D = 5, 12 mm diameter (c) L/D = 5, 16 mm diameter (d) L/D = 5, 20 mm diameter

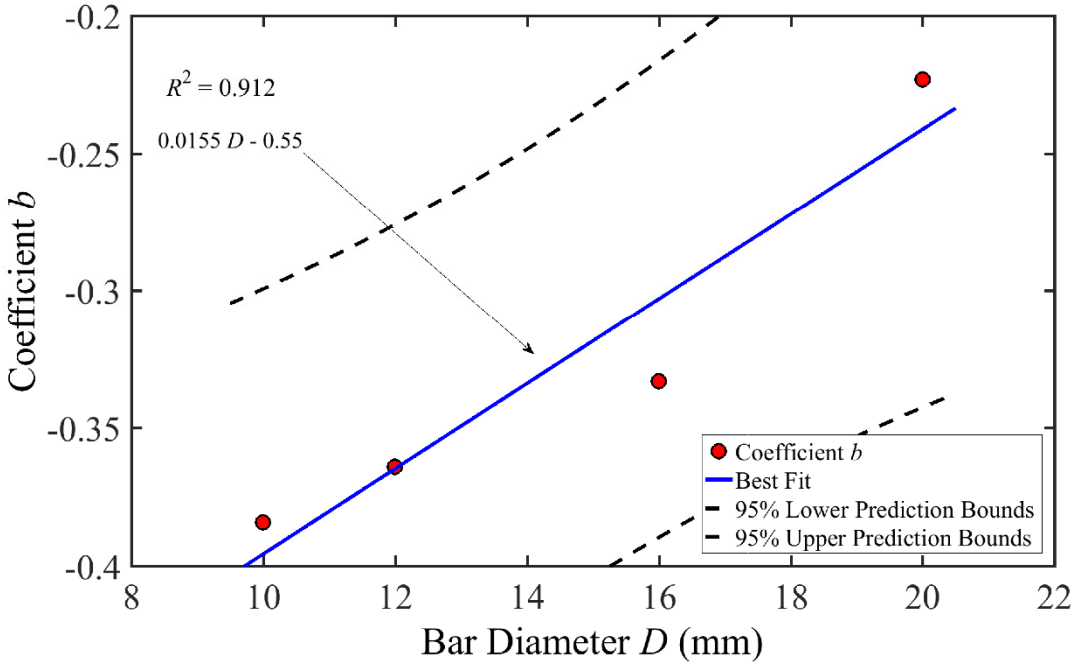

(a)

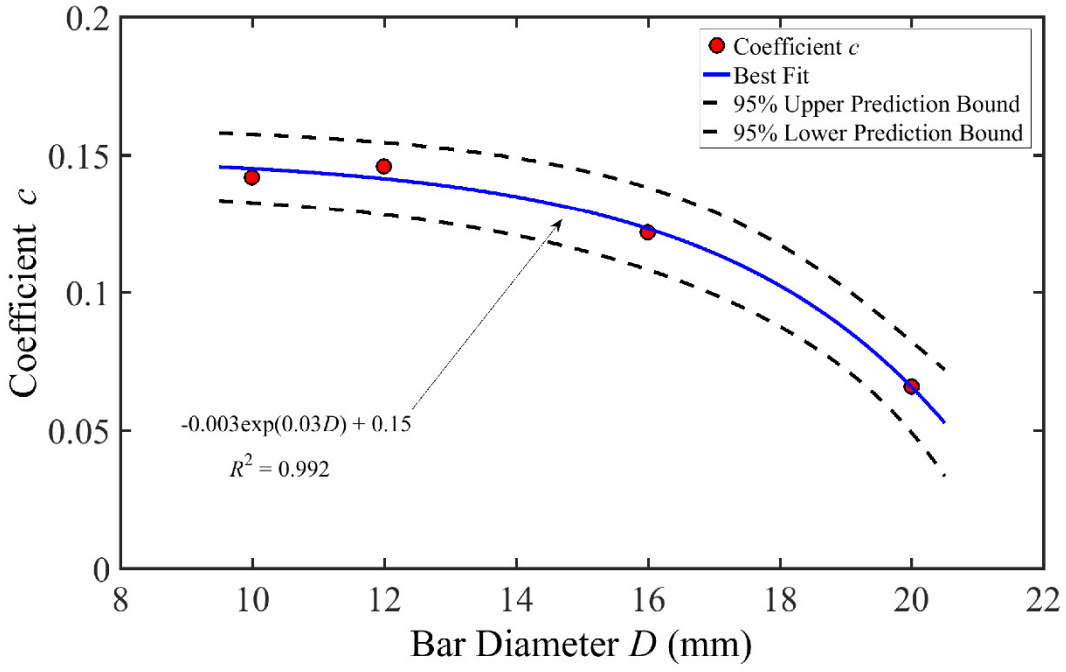

(b)

Figure 5: Influence of bar diameter on fatigue material constants: (a) empirical coefficient *b* in Table 2 (b) empirical coefficient *c* in Table 2

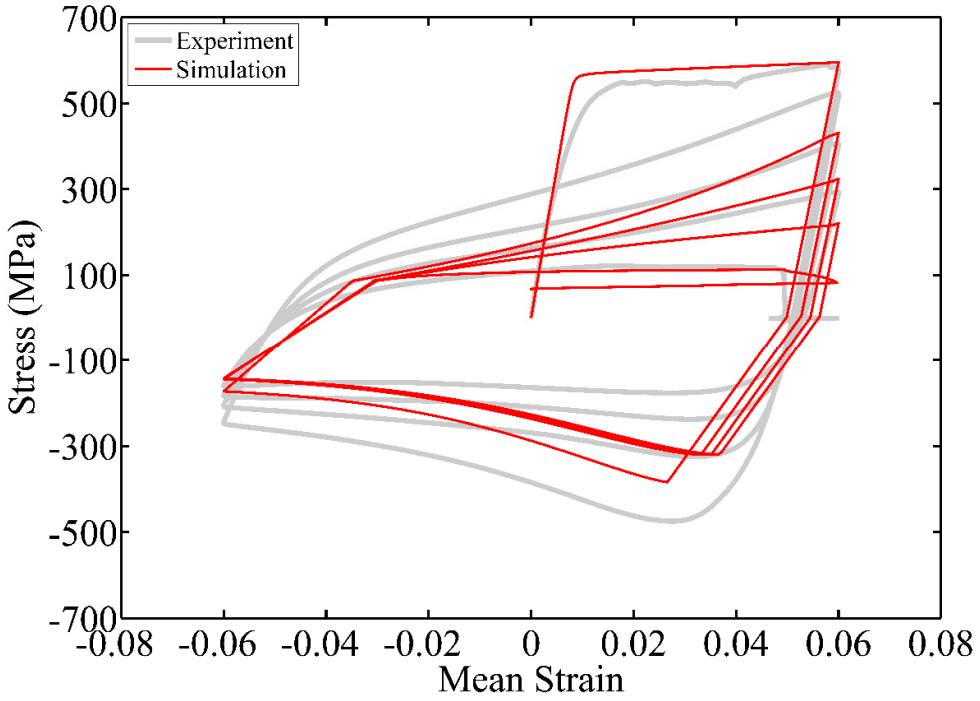

(a)

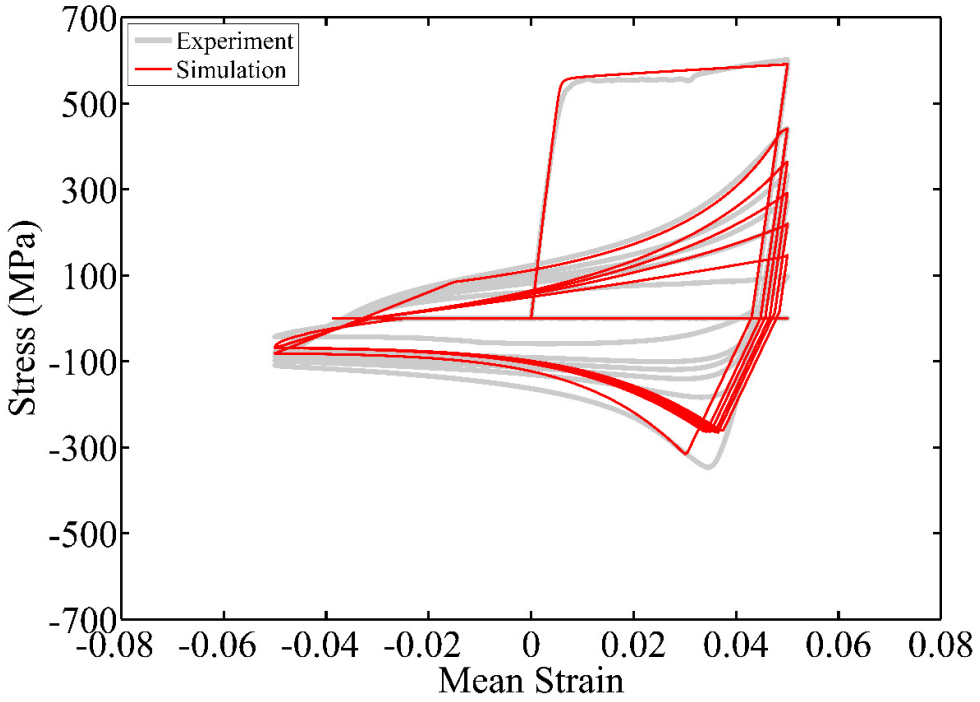

(b)

Figure 6: Comparison of simulation results using the constitutive model proposed in (Kashani et al. 2015b) and observed experimental results for 20 mm diameter bars with L/D = 8 (a) and 15 (b) respectively

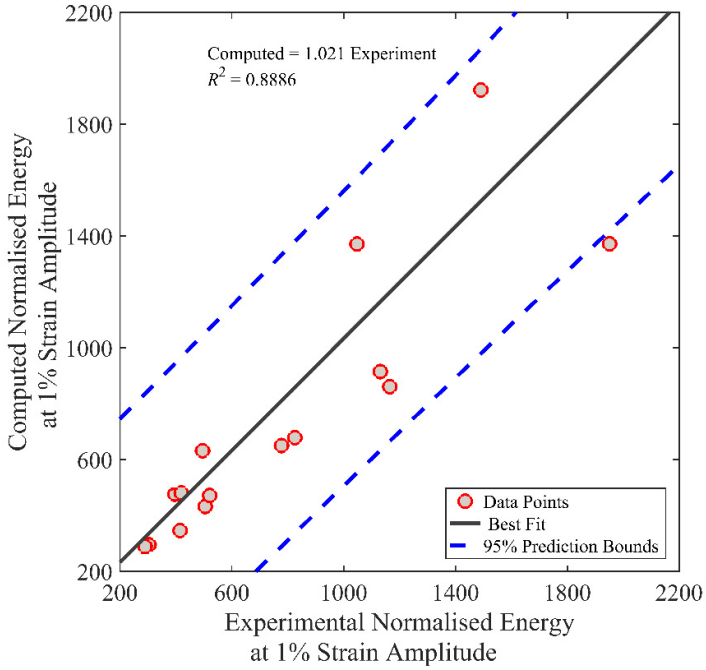

(a)

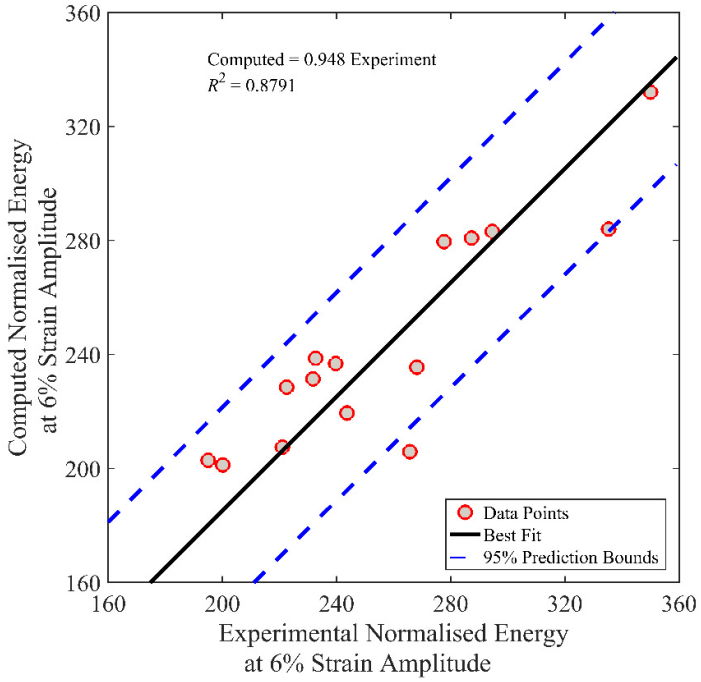

(b)

Figure 7: Comparison of computed and experimental normalised hysteretic energy of all the bars with $L/D \geq 8$: (a) 1% strain amplitude, and (b) 6% strain amplitude

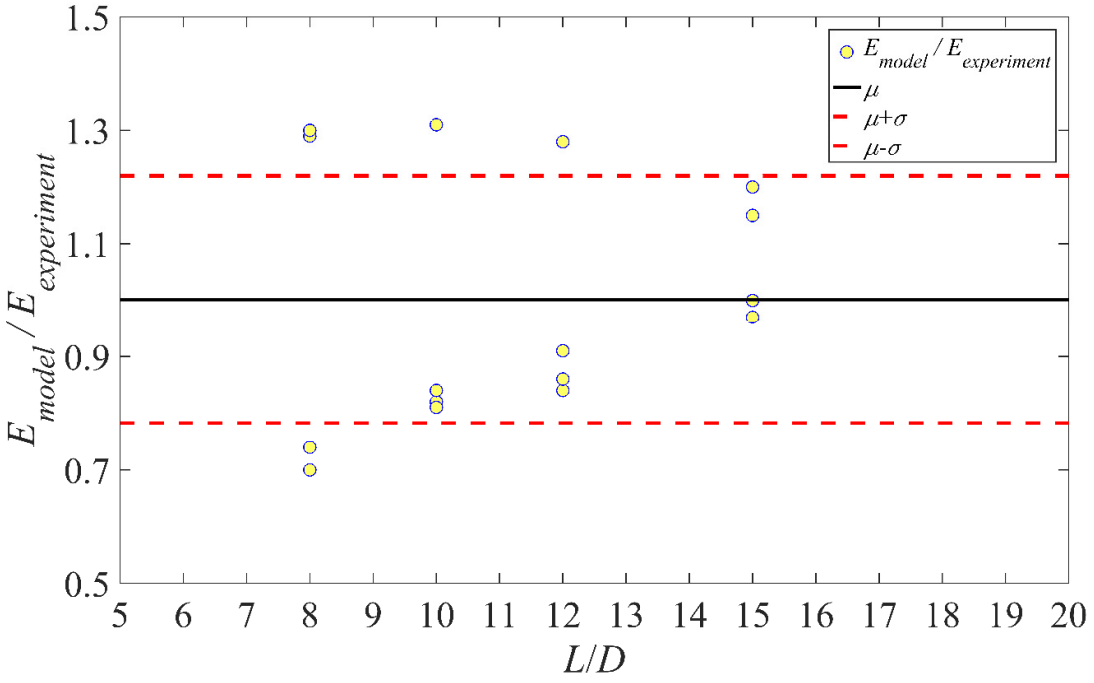

(a)

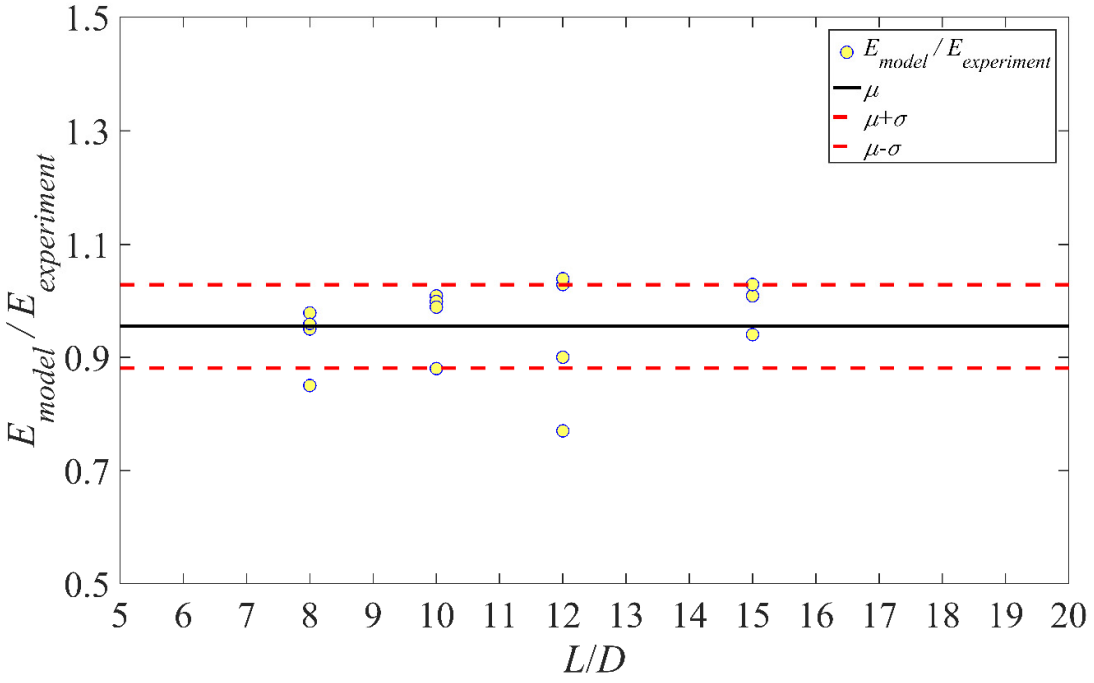

(b)

Figure 8: Mean and standard deviation of ratio of E_t/E_y of all the bars with $L/D \geq 8$: (a) 1% strain amplitude, and (b) 6% strain amplitude